ACS Sustainable Chemistry & Engineering

Research Article

pubs.acs.org/journal/ascecg

Acrylic Triblock Copolymers Incorporating Isosorbide for Pressure Sensitive Adhesives

James J. Gallagher, Marc A. Hillmyer,* and Theresa M. Reineke*

Department of Chemistry, University of Minnesota, 207 Pleasant St SE, Minneapolis, Minnesota 55455-0431, United States

Supporting Information

ABSTRACT: A new monomer acetylated acrylic isosorbide (AAI) was prepared in two steps using common reagents without the need for column chromatography. Free radical polymerization of AAI afforded poly(acetylated acrylic isosorbide) (PAAI), which exhibited a glass transition temperature (T_g) = 95 °C and good thermal stability (T_d, 5% weight loss; N_2 = 331 °C, air = 291 °C). A series of ABA triblock copolymers with either poly(*n*-butyl acrylate) (PnBA) or poly(2-ethylhexyl acrylate) (PEHA) as the low T_g midblocks and PAAI as the high T_g end blocks were prepared using Reversible Addition−Fragmentation chain Transfer (RAFT) polymerization. The triblock copolymers ranging from 8−24 wt % PAAI were evaluated as pressure sensitive adhesives by 180° peel, loop tack, and static shear testing. While the PAAI-PEHA-PAAI series exhibited poor adhesive qualities, the PAAI-PnBA-PAAI series of triblock copolymers demonstrated peel forces up to 2.9 N cm^{-1}, tack forces up to 3.2 N cm^{-1}, and no shear failure up to 10 000 min. Dynamic mechanical analysis indicated that PAAI-PEHA-PAAI lacked the dissipative qualities needed to form an adhesive bond with the substrate, while the PAAI-PnBA-PAAI series exhibited a dynamic mechanical response consistent with related high performing PSAs.

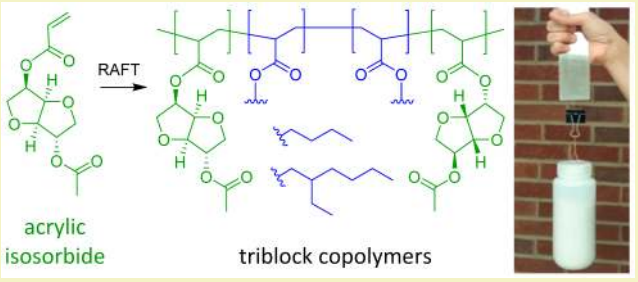

KEYWORDS: *Renewable, RAFT, High T_g, Thermoplastic elastomer, Butyl acrylate, 2-Ethylhexyl acrylate*

INTRODUCTION

Polymers derived from renewable resources have recently experienced a remarkable resurgence due to long-term environmental and availability concerns associated with petroleum derivatives.[1−4] The bicyclic sugar derivative isosorbide has garnered much attention as a biobased feedstock for polymer applications and has become available on a commercial scale as a result of improvements in production technology.[5] For example, the French agricultural company Roquette recently completed the world's largest isosorbide production plant capable of producing 20 000 tons annually of high purity polymer grade isosorbide.[6] Incorporating isosorbide into a polymer imparts desirable qualities such as high glass transition temperature (T_g) and thermal stability (as characterized by the temperature at 5% mass loss, T_d). The diol functionality of isosorbide naturally lends itself to use in step growth polymers such as polyesters, polyurethanes, and polycarbonates. The application of isosorbide and the related dianhydrohexitols isomannide and isoidide in this area has been extensively studied.[7−9] An example of a commercial isosorbide based polymer is Mitsubishi's poly(isosorbide carbonate) product Durabio, which finds use in automotive and electronic display applications due to its superior durability and optical clarity.[10,11]

A distinct advantage of controlled chain growth polymerization over step growth polymerizations is the ability to achieve narrow molar mass distributions and well-defined polymer architectures. However, only a few reports have focused on using isosorbide in chain growth polymerizations.[12−16] We previously described the preparation of a new monofunctional methacrylic isosorbide monomer (AMI) and its incorporation into block copolymers by Reversible Addition−Fragmentation chain Transfer (RAFT) polymerization.[12] Preparation of PAMI samples from different monomer regioisomer compositions showed that regiochemistry did not have a significant impact on polymer properties. Macro chain transfer agents of PAMI were prepared with a narrow molar mass distribution ($Đ$) and controlled number-average molar mass (M_n). Subsequent chain extension with *n*-butyl acrylate afforded a series of well-defined PAMI-PnBA diblock copolymers. Likewise, the synthesis of vinyl triazole monomers derived from isosorbide, isomannide, and isoidide and the polymerization thereof using RAFT polymerization has also been reported.[13] It was shown that the regiochemistry of poly vinyl triazoles from isosorbide had a significant impact on T_g and water solubility.

The ability to incorporate isosorbide into block polymers is appealing because it expands the scope of potential applications for this biobased feedstock. Block copolymers find use as toughening agents, thermoplastic elastomers, and pressure

Received: March 3, 2016
Revised: April 23, 2016
Published: May 10, 2016

DOI: 10.1021/acssuschemeng.6b00455
ACS Sustainable Chem. Eng. 2016, 4, 3379−3387

sensitive adhesives (PSAs).[17] When the traditional poly(styrene)-poly(isoprene)-poly(styrene) block polymers are used as PSAs, it is necessary to compound them with midblock miscible tackifiers.[18] Tackifiers effectively increase the entanglement molecular weight (M_e) of the midblock and thus lower the storage modulus of the elastomer, which would otherwise be too high to allow intimate contact with a substrate to form an adhesive bond.[18] Acrylic block copolymers have been investigated as an alternative to styrenic block copolymers for various applications.[19−24] The most prominent example of an acrylic block copolymer is poly(methyl methacrylate)-poly(*n*-butyl acrylate)-poly(methyl methacrylate) (PMMA-PnBA-PMMA).[20,24] The commercial grade version of this triblock copolymer is produced by Kuraray Co., Ltd. for use in PSA applications as Kurarity LA2140e. Unlike styrenic block copolymers, PMMA-PnBA-PMMA can be used with or without tackifier for PSA applications.[23] The M_e of PnBA is ∼5−10 times higher than poly(butadiene) or poly(isoprene), resulting in a storage modulus that is inherently low enough to form an adhesive bond. Moreover, acrylic block copolymers have certain advantages over styrenic block copolymers such as UV light and oxidation resistance. Acrylics also have more functional versatility due to the ability to vary the pendant ester group without significantly altering the reactivity of the acrylate moiety. As a result polyacrylates can exhibit an exceptionally broad range of polarity and T_g values.[25]

Supplementing petroleum derived feedstocks with biobased resources is a vital aspect to improving the sustainability of PSAs.[26] Previous reports describing sustainable triblock copolymers for PSA applications focused on the ring opening polymerization of biobased lactones to afford the corresponding polyesters.[27−30] Similar to the styrenic block copolymers, PSA formulations featuring the triblock copolyesters required addition of tackifier due to the relatively low M_e of the, for example, poly(menthide) and poly(ε-caprolactone) midblocks. Results from adhesion testing of the triblock copolyester and tackifier formulations demonstrated performance similar to commercial PSAs. Renewably sourced acrylates have also been reported for use in PSA applications.[26] For example, Severtson and co-workers described a platform based on acrylic functionalized poly(lactide-*co*-caprolactone) and random copolymers thereof with various (meth)acrylic comonomers.[31−33] An example of a PSA system incorporating isosorbide was recently described by Vendamme and Eevers.[34] The PSAs were prepared by polycondensation between isosorbide and a dimerized fatty acid followed by thermal curing of the resultant polyester with epoxidized plant oils. The researchers reported an increase in T_g and peel force for the PSAs incorporating isosorbide over those derived from dimerized fatty alcohols.

In this work we endeavored to expand the utility of isosorbide by incorporating it into an all acrylic triblock copolymer via a controlled chain growth polymerization. To this end, we detail (i) synthesis of a new monomer acetylated acrylic isosorbide (AAI) in two steps from common reagents without the need for chromatographic separations; (ii) free radical polymerization of AAI to afford a thermally stable and high T_g thermoplastic PAAI; (iii) incorporation of PAAI into well-defined triblock copolymers with low T_g acrylic midblocks via RAFT polymerization; and (iv) evaluation of PSA performance as a function of PAAI content and midblock structure.

RESULTS AND DISCUSSION

Synthesis of AAI. AAI was prepared in two steps according to Scheme 1a. In the first step, the monoacetate was prepared by esterification of isosorbide with acetic acid, followed by a tandem transesterification−distillation step to afford isosorbide *exo* acetate in a crude yield of 69%. After recrystallization from methyl ethyl ketone, the purified product was obtained in a 38% yield. While the yield on a per distillation basis was modest in our hands, the yield can be increased by resubjecting the mother liquor to the reactive distillation process. Additional improvements in the yield could be achieved by using a distillation column with more theoretical plates. This method for preparing isosorbide *exo* acetate was first reported by Stoss[35,36] and is remarkable for its ability to provide an isosorbide monoacetate in good yield and high purity. Furthermore, this route utilizes common reagents and minimal solvent making it particularly appealing for scalable production. The acrylate moiety was then installed by esterifying the pure monoacetate with acryloyl chloride to afford AAI as a crystalline solid.

Scheme 1. Synthesis of AAI[a]

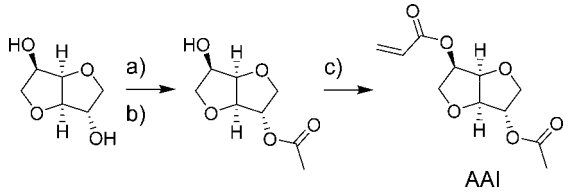

[a](a) 1.3 mol eq acetic acid, 1 wt % *p*-toluenesulfonic acid, refluxed toluene, Dean-Stark trap. (b) 2 wt % KOH, 200 mTorr, reactive distillation. (c) 1.05 mol eq acryloyl chloride, 1.1 mol eq triethylamine, 0 °C to r.t., 18 h, DCM.

The structure of AAI was confirmed by NMR and IR spectroscopy. The acrylic protons are clearly visible in the ^{1}H NMR spectrum between 6.47 and 5.81 ppm (Figure S1) and the vinyl carbons appear in the ^{13}C NMR spectrum at 132 and 128 ppm (Figure S2). The presence of only one set of resonances in the NMR spectra indicates that only the *exo*-acyl-*endo*-acryloyl-isosorbide isomer is present in the product. The acrylic moiety is also indicated by the vibrations at 1726 cm^{-1} (C═O) and 1637 cm^{-1} (C═C) in the IR spectrum (Figure S3). Further structural confirmation was provided by high-resolution mass spectrometry ([M + Na$^+$] expected =265.0688; found: 265.0684; error 1.51 ppm).

The thermal properties of AAI were investigated using thermogravimetric analysis (TGA) and differential scanning calorimetry (DSC). Two mass loss events were observed by TGA of AAI in N_2 and air (Figure S4). The onset of the first mass loss occurred at a higher temperature (152 °C) under air and constituted a smaller mass loss (6 wt %) than the result in N_2 (148 °C and 21 wt %) likely due to the *in situ* polymerization of AAI during TGA in the presence of oxygen. This hypothesis is supported by the TGA result in the presence of the free radical inhibitor butylated hydroxytoluene where 95% of the mass loss occurs during the first mass loss event, indicating that polymerization was suppressed. DSC of AAI was used to determine a melting point and T_g of 38 and −36 °C, respectively (Figure S5). A difference of ∼100 °C between the melting point and onset of degradation of AAI indicates this

DOI: 10.1021/acssuschemeng.6b00455
ACS Sustainable Chem. Eng. 2016, 4, 3379−3387

Scheme 2. Synthesis of PAAI-PnBA-PAAI and PAAI-PEHA-PAAI by RAFT Polymerization

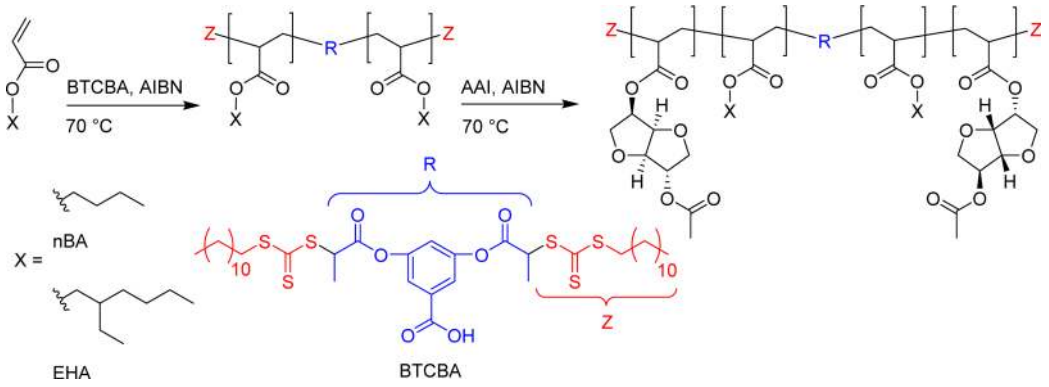

Table 1. PAAI-PnBA-PAAI and PAAI-PEHA-PAAI Molar Mass Data

polymer	[M]/[CTA][a]	time (h)	conv (%)	M_n (calc)[b] (kg mol^{-1})	M_n (SEC)[c] (kg mol^{-1})	M_n (NMR)[d] (kg mol^{-1})	$Đ$[c]	PAAI[e] (wt %)
PnBA 27k	100	2	86	22.0	27.4	25.8	1.06	0
PAAI-PnBA-PAAI (63k, 54%)	94	2	68	58.4	63.2	52.1	1.19	54
PnBA 45k	250	2	69	44.2	45.3	44.4	1.03	0
PAAI-PnBA-PAAI (53k, 12%)	39	1.5	34	51.7	53.3	49.8	1.09	12
PAAI-PnBA-PAAI (60k, 17%)	39	2	57	56.1	60.2	65.6	1.12	17
PAAI-PnBA-PAAI (70k, 21%)	55	2.5	48	59.5	69.2	67.5	1.15	21
PEHA 45k	115	1	90	38.1	44.7	43.4	1.06	0
PAAI−PEHA-PAAI (51k, 8%)	14	2	58	58.5	51.3	51.3	1.18	7.9
PAAI-PEHA-PAAI (54k, 14%)	22	2	70	52.2	54.2	52.3	1.2	14
PAAI-PnBA-PAAI (64k, 24%)	36	2	79	48.6	63.5	60.9	1.25	24

[a]CTA defined as trithiocarbonate moiety (i.e., 2 CTA per BTCBA), [CTA]:[AIBN] = 10:1. [b]Assuming 1 BTCBA molecule per polymer chain (see SI). [c]From SEC-MALLS in THF. [d]Determined relative to aromatic mid group. [e]From ^{1}H NMR spectroscopy.

monomer can be processed in the liquid state without incurring degradation.

Free Radical Polymerization of AAI. A sample of PAAI prepared by normal free radical polymerization (Scheme S1, Figure S6) was soluble at 10 wt % in THF, ethyl acetate, CH_2Cl_2, $CHCl_3$, acetone, and DMF but was insoluble in water, MeOH, ether, and hexanes. Size exclusion chromatography with multiangle laser light scattering detection (SEC-MALLS) in THF was used to determine a number-average molar mass (M_n) = 120 kg mol^{-1} and a molar mass distribution ($Đ$) = 4.00 (Figure S7). Thermal degradation temperatures (T_d, 5 wt % loss) of PAAI under N_2 and air were determined by TGA to be 337 and 291 °C, respectively, while DSC analysis showed a T_g = 95 °C (Figures S8 and S9). The thermal stability of PAAI is significantly higher than that reported for PAMI prepared by free radical polymerization (T_d, 5 wt % loss; N_2 = 251 °C, air = 217 °C). The higher T_d of PAAI supports our previous hypothesis that the onset of thermal degradation of PAMI was due to the instability of the methacrylic backbone rather than that of the pendant isosorbide groups.[12] Polymethacrylates undergo thermal decomposition at ∼200−250 °C due the favorable depolymerization of the polymer backbone, while polyacrylates typically degrade at ∼300−350 °C via a random chain scission mechanism.[37,38] The similar T_d of PAAI to other polyacrylates exemplifies the desirable thermal stability of isosorbide. The T_g of PAAI is lower than what was previously reported for PAMI (T_g = 130 °C) due to the increased flexibility of the polyacrylic backbone relative to the polymethacrylic backbone. Nevertheless, the steric bulk of the pendant isosorbide acetate groups of PAAI impart enough rigidity to afford a T_g within the realm of typical glassy polymers such as PMMA and poly(styrene) (T_g ∼ 110 and 100 °C, respectively).

PAAI-PnBA-PAAI and PAAI-PEHA-PAAI via RAFT Polymerization. RAFT polymerization was selected as a means to prepare the desired triblock copolymers.[39,40] To determine the appropriate RAFT agent for controlled polymerization of AAI, a series of RAFT chain transfer agents (CTAs) were screened (Table S1). Trithiocarbonates 1 and 2 afforded PAAI with $Đ \leq 1.20$ and a M_n (SEC) within 5% error of M_n (calc), while no significant polymerization of AAI was observed with dithiobenzoates 3 and 4 after 18 h. Dithiobenzoates have been reported to inhibit polymerization of acrylates due to their low rate of fragmentation.[41] Therefore, the commercially available CTA 3,5-bis(2-dodecylthiocarbonothioylthio-1-oxo-propoxy)benzoic acid (BTCBA) was selected to construct the desired library of triblock copolymers. While there are no reports of BTCBA being used in the open literature the butyl trithiocarbonate analogue has been reported to successfully control the polymerization of nBA.[42] A distinct advantage of BTCBA over other monofunctional RAFT CTAs is the ability to construct the desired ABA triblock in only two consecutive polymerization steps.

2-Ethylhexyl acrylate (EHA) and nBA were selected to construct the midblock portion of the triblock copolymers. Both monomers are commercially available, inexpensive, and find extensive use as low T_g components in polyacrylates.[43] Acrylics are particularly attractive from a sustainability point of view as the development of biobased acrylic acid has been actively pursued.[44] The monomer nBA is also appealing due to

DOI: 10.1021/acssuschemeng.6b00455
ACS Sustainable Chem. Eng. 2016, 4, 3379−3387

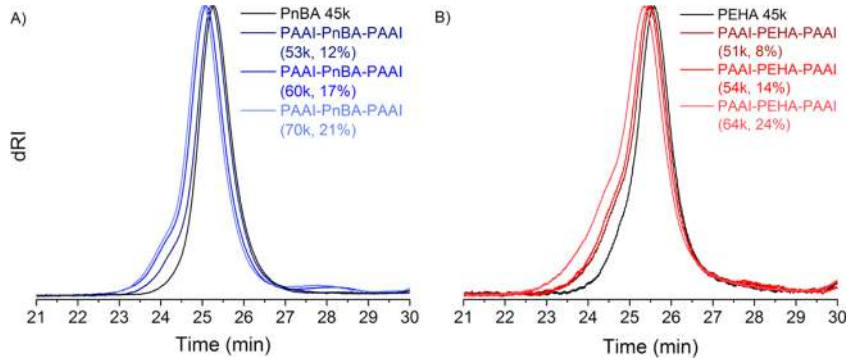

Figure 1. THF SEC with differential refractive index (dRI) detector of (A) PAAI-PnBA-PAAI and (B) PAAI-PEHA-PAAI triblock copolymers used for adhesion testing.

the potential for biosourced *n*-butanol.[26] Furthermore, PEHA is known to have good film formation properties.[45] PnBA and PEHA have distinct M_e values (28 and 59 kg mol^{-1}, respectively) allowing us to determine the effect of midblock structure on the adhesive performance of the materials. nBA and EHA were polymerized neat in the presence of BTCBA and AIBN at 70 °C to afford the corresponding macro-CTAs (Scheme 2, Table 1). ^{1}H NMR analysis confirmed the presence of the expected mid and end groups (Figures S10 and S11). Resonances at 7.68 and 7.13 ppm correspond to the aryl mid group protons, the tertiary proton of the terminal repeat unit appears at 4.82 ppm, and the α methylene protons of the trithiocarbonate are visible at 3.33 ppm. No significant difference was observed for the mid and end group resonances between PnBA and PEHA. The observed resonances were in excellent agreement with those reported previously for the butyl trithiocarbonate analogue.[42] M_n (NMR) and M_n (SEC) were also in good agreement (Table 1) and $Đ$ < 1.06 was achieved for all three macro-CTAs indicating good control of the RAFT polymerization.

Chain extension of the PnBA and PEHA macro-CTAs with AAI afforded the triblocks PAAI-PnBA-PAAI and PAAI-PEHA-PAAI, respectively. An advantage of AAI over AMI is that acrylic monomers can be used for controlled chain extension via RAFT from an acrylic macro-CTA while methacrylic monomers cannot.[40] To first demonstrate a controlled chain extension reaction, PnBA 27k was used as a macro-CTA to prepare a sample of PAAI-PnBA-PAAI with 54 wt % PAAI. A clear shift to lower elution volume in the SEC trace indicated successful chain extension (Figure S12). A high molar mass shoulder was present in the SEC trace of the triblock likely due to termination by combination, however the molar mass distribution was relatively narrow ($Đ$ = 1.19) suggesting that the chain extension reaction was well controlled. M_n (SEC) was 63.2 kg mol^{-1} in good agreement with the theoretical M_n (calc) (58.4 kg mol^{-1}). The aromatic mid group and α methylene protons of the trithiocarbonate end group were visible in the ^{1}H NMR spectrum at the same chemical shifts as for PnBA 27k (Figure S13). The terminal repeat unit tertiary proton was no longer visible as it was obscured by the PAAI repeat unit resonances. Two series of triblock copolymers to be evaluated as pressure sensitive adhesives were then prepared by chain extension of PnBA 45k and PEHA 45k. Different lengths of the PAAI end block were prepared by varying the ratio of CTA to AAI during the polymerization. The M_n (SEC) in kg mol^{-1} and weight percent of PAAI as determine by NMR are indicated for each sample (Table 1). Again, a shift in the peak in the SEC trace to lower elution times (Figure 1) and $Đ$ < 1.25 was maintained for all triblock copolymers indicating successful chain extension. The wt % of PAAI ranged from 8−24 consistent with typical hard block composition for triblock copolymers in PSA applications.[23,27−29]

Alcoholysis was performed on a sample of triblock to confirm symmetric growth from the central initiating fragment. PAAI-PnBA-PAAI (60k, 17%) was heated to 130 °C in the presence of *p*-toluenesulfonic acid and excess *n*-butanol for 48 h (Scheme S2). ^{1}H NMR analysis after purification by precipitation and drying showed no aromatic resonances corresponding to the mid group, indicating full alcoholysis of the benzylic esters (Figure S14). Trace amounts of broad resonances between 3.75 and 5.25 ppm suggest some residual pendant isosorbide groups. The chemical shifts do not match that of PAAI and likely correspond to a deacetylated isosorbide group. On the basis of peak integration relative to PnBA the residual isosorbide pendant groups are estimated to be present at <5 wt %. The SEC trace of PAAI-PnBA-PAAI (60k, 17%) after alcoholysis was monomodal with M_n = 35.4 kg mol^{-1}, near the expected value of 30.1 kg mol^{-1} (Figure S15). Thus, we conclude that RAFT polymerization allowed preparation of two series of triblock copolymers in two steps with good control over molar mass composition and a symmetric polymer architecture.

Thermal, Morphological, and Mechanical Characterization of Triblock Copolymers. PAAI-PnBA-PAAI (60k, 17%) and PAAI-PEHA-PAAI (54k, 14%) exhibited similar thermal stability under N_2 (T_d = 334 and 338 °C, respectively) (Figures S16 and S17). Thermal stability in the presence of oxygen however differed significantly between the two samples. PAAI-PnBA-PAAI (60k, 17%) had a higher thermal stability in air (T_d = 304 °C) than PAAI-PEHA-PAAI (54k, 14%) (T_d = 264 °C). The onset of degradation for PAAI-PEHA-PAAI (54k, 14%) at lower temperature may be due to the tertiary carbons present in the PEHA pendant groups, which are prone toward oxidative degradation. DSC analysis of the triblocks showed T_g values corresponding to PnBA and PEHA midblocks at ∼−45 and −60 °C, respectively (Figure 2). With the exception of PAAI-PnBA-PAAI (63k, 54%) which exhibited two T_g values at −45 and 80 °C, no clear transition could be assigned to the T_g of the PAAI end blocks in the other block copolymer samples. A potential explanation is that the DSC is not sensitive enough to determine the T_g of the end blocks due to their low weight percent present in each sample. The presence of midblock T_g near that of the homopolymer and independent of weight percent PAAI suggests that the two polymer components are not mixed. For example, based on homopolymer T_g of −65 and

DOI: 10.1021/acssuschemeng.6b00455
ACS Sustainable Chem. Eng. 2016, 4, 3379−3387

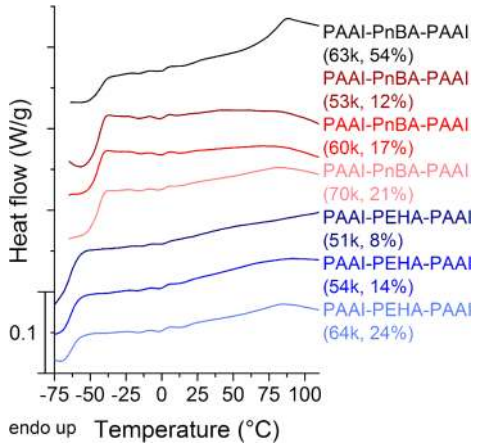

Figure 2. DSC of PAAI-PnBA-PAAI and PAAI-PEHA-PAAI triblock copolymers. Heating rate = 10 °C min^{-1}, 2nd heating. Data are shifted vertically for clarity.

95 °C and assuming the two components are mixed, the Fox equation predicts T_g for PAAI-PEHA-PAAI (51k, 8%) = −57 °C and PAAI-PEHA-PAAI (64k, 24%) = −41 °C.

Small angle X-ray scattering (SAXS) was used to probe the phase separation of the triblock copolymers (Figure 3). The

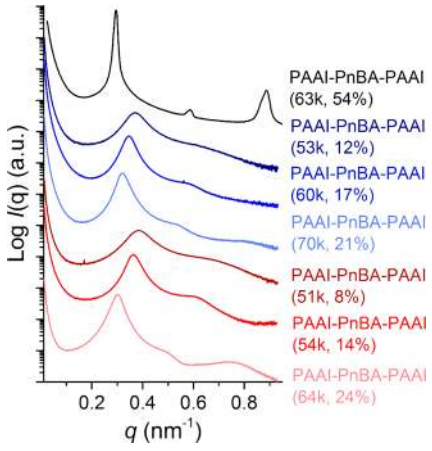

Figure 3. SAXS patterns for PAAI-PnBA-PAAI and PAAI-PEHA-PAAI triblock copolymers. Data are shifted vertically for clarity.

scattering profile of PAAI-PnBA-PAAI (63k, 54%) confirmed the expected lamellar morphology of this sample with peaks distinctly visible at integer multiples of the principle scattering peak (q^*). The scattering profiles of triblocks with lower PAAI content exhibited a q^* and not well-defined secondary peaks. The broad nature of the higher order peaks precludes the definitive assignment of the morphology of these samples, however other reports of similar scattering patterns from triblocks with low end block content have been claimed to indicate a spherical morphology with limited long-range order.[29,30] The principle domain spacing ($D^* = 2\pi/q^*$) of the triblock copolymer samples ranged from 16.3−20.8 nm, and the sphere radii were estimated to be between 4.5−7.9 nm based on fitting a spherical form factor to the SAXS scattering profiles (Table S2).

The mechanical properties of an elastomer play an important role in PSA performance. Elastomers that exhibit low toughness tend to fail within the elastomer layer and leave residue on the adherend (cohesive failure), while tougher elastomers tend to fail at the interface between adherend and elastomer without leaving residual material on the adherend (adhesive failure). Adhesive failure is required for removable PSAs such as masking tape, whereas cohesive failure is desirable for permanent PSA applications such as labels and packaging. To this end, the mechanical properties of PAAI-PnBA-PAAI (60k, 17%) and PAAI-PEHA-PAAI (54k, 14%) were evaluated using tensile testing (Figure 4). Significant differences were observed

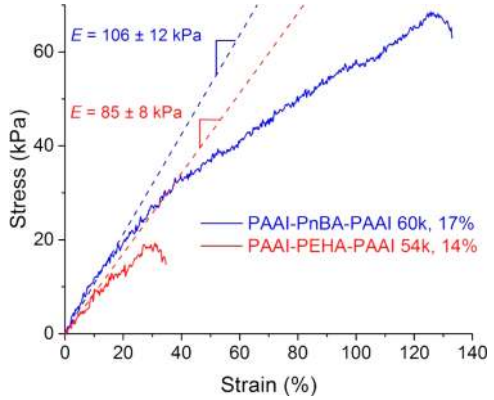

Figure 4. Representative stress vs strain curves for PAAI-PnBA-PAAI (60k, 17%) and PAAI-PEHA-PAAI (54k, 14%). Moduli are averages of five samples; see Figures S18 and S19.

in the stress vs strain curves between the two triblocks. Young's moduli (E) of PAAI-PnBA-PAAI (60k, 17%) and PAAI-PEHA-PAAI (54k, 14%) were 106 ± 12 and 85 ± 8 kPa, respectively. PAAI-PnBA-PAAI (60k, 17%) also displayed higher elongation at break, stress at break, and toughness than PAAI-PEHA-PAAI (54k, 14%). All samples tore at the grips of the tensile tester rather than in the gauge region, therefore preventing the quantitative description of the ultimate tensile behavior of these samples. However, because the samples were all tested under the same conditions, the qualitative difference between the two polymer samples is notable. Higher values of E and toughness for PAAI-PnBA-PAAI (60k, 17%) are a result of the lower M_e of PnBA relative to PEHA. At a midblock length of 45 kg mol^{-1} PnBA is expected to be moderately entangled, while PEHA should be unentangled. The lack of entanglements to dissipate the applied tensile stress results in relatively poor mechanical properties. Commercial PSA grade PMMA-PnBA-PMMA triblock copolymer with 23 wt % PMMA was reported to have E = 1.00 MPa and tensile strength = 6.24 MPa,[27] however the unknown molar mass of the commercial sample precludes any useful comparison to the properties reported above for PAAI-PEHA-PAAI (54k, 14%) and PAAI-PnBA-PAAI (60k, 17%). The polyester triblocks previously reported for use as PSAs showed even higher values of E and tensile strength (up to 5.97 and 13.6 MPa, respectively) due to the high molar mass and low midblock M_e.[27−29]

Adhesive Performance of Triblock Copolymers. The adhesives were prepared by dissolving the polymer in ethyl acetate and solution coating onto a sheet of poly(ethylene terephthalate) using a wound wire rod. The films were then left to dry under ambient conditions for 24 h before testing. The adhesive performance of the triblock copolymers was evaluated by 180° peel, loop tack, and static shear tests (Figure 5, Figures S20−S29). A significant difference was observed in the 180° peel test results between the PAAI-PnBA-PAAI and PAAI-PEHA-PAAI series of polymers. The PAAI-PEHA-PAAI series

DOI: 10.1021/acssuschemeng.6b00455
ACS Sustainable Chem. Eng. 2016, 4, 3379−3387

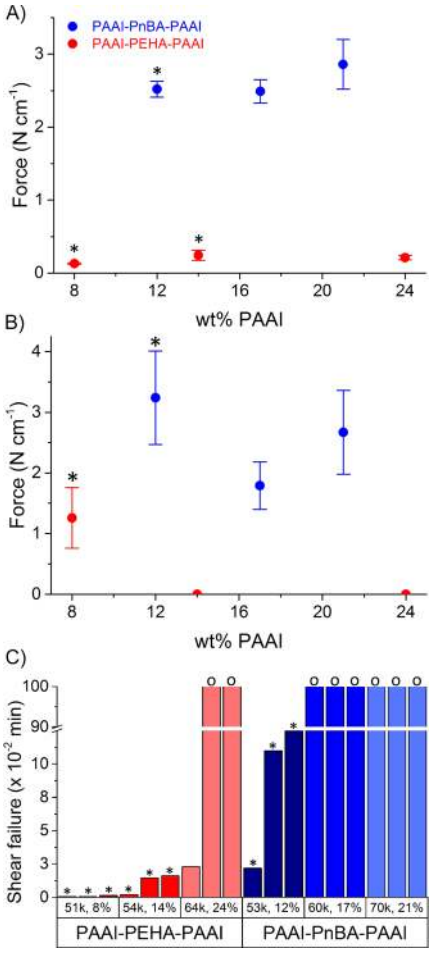

Figure 5. Adhesive performance of PAAI-PnBA-PAAI and PAAI-PEHA-PAAI triblock copolymers. (A) 180° peel test; (B) loop tack test; (C) shear test. Each bar represents one sample. * = cohesive failure, ○ = no failure after 10 000 min.

exhibited average peel forces in the range of 0.13 to 0.24 N cm^{-1}, with no significant differences observed between samples with 8, 14, and 24 wt % PAAI. Cohesive failure was observed for PAAI-PEHA-PAAI (51k, 8%) and (54k, 14%) as expected due to its rather low toughness. Similar values of peel adhesion are reported for excellent removable types of adhesives, however the cohesive mode of failure is unacceptable for removable PSAs. By contrast, average values of peel adhesion for the PAAI-PnBA-PAAI series of polymers ranged from 2.5 to 2.9 N cm^{-1}. Similar peel force values of ∼1−3 N cm^{-1} for commercially available PMMA-PnBA-PMMA triblock copolymers have been previously reported.[23,46] Other than the cohesive failure observed for PAAI-PnBA-PAAI (53k, 12%) no significant difference was observed across the range of different wt % of PAAI. Loop tack testing also produced significantly different results between the two sets of polymers. PAAI-PEHA-PAAI (51k, 8 wt %) was the only sample among the PAAI-PEHA-PAAI series that was able to form a bond to the stainless steel substrate during testing. The other samples formed no interaction with the substrate and did not register a force during loop tack testing. All samples in the PAAI-PnBA-PAAI series registered an average tack force between 1.8 and 3.2 N cm^{-1}. The shear test results indicated that the PAAI-PnBA-PAAI series showed good resistance to shear failure, particularly the samples with 17 and 21 wt % PAAI which showed no failure after 10 000 min. PAAI-PEHA-PAAI (51k, 8 wt %) and (54k, 14%) showed poor shear resistance with failure occurring in less than 200 min. Results from the shear test of PAAI-PEHA-PAAI (64k, 24%) were inconsistent across the three samples tested, with one failure occurring at 230 min and no failure observed after 10 000 min for the other two.

Polymers for adhesive applications are typically blended with additives such as tackifiers and plasticizers to tune adhesive properties and processability. For example, addition of a tackifier can impact adhesive performance by increasing T_g and dissipative qualities.[47] To improve the tack and peel forces of PEHA based series of polymers, PAAI-PEHA-PAAI (54k, 14%) was blended with 25 and 50 wt % of a rosin ester tackifier. Rosin esters are commonly used as tackifiers for adhesives and have the added benefit of being renewably derived.[48] After solvent casting and drying under ambient conditions for 24 h, the resulting polymer films appeared homogeneous and clear, indicating good compatibility between the tackifier and polymer. DSC showed an increase in T_g from −63 to −21 °C with increasing weight percent of the tackifier (Figure S30). Both tack and peel forces increased significantly with increasing tackifier content (Figures 6, S31−34). Cohesive failure was

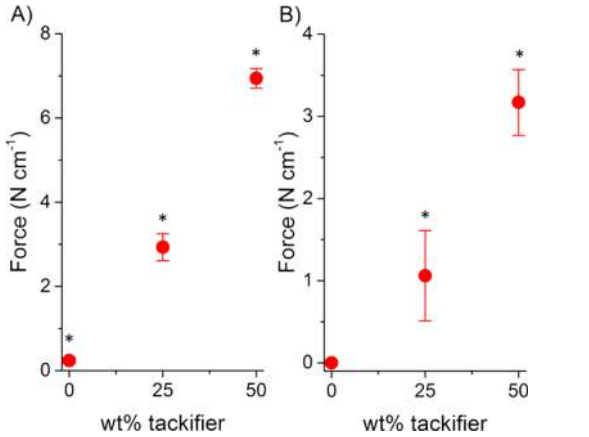

Figure 6. Adhesion testing of PAAI-PEHA-PAAI (54k, 14%) plus rosin ester tackifier: (A) loop tack test; (B) 180° peel test; * = cohesive failure.

observed in both the loop tack and 180° peel experiments due to the poor toughness of the base elastomer. With a peel force >4 N cm^{-1} and cohesive mechanism of failure, PAAI-PEHA-PAAI (54k, 14%) with 50 wt % tackifier fits the definition of a permanent PSA.[49]

Dynamic Mechanical Analysis. To gain insight into the cause for the dramatic differences in adhesive qualities between PAAI-PEHA-PAAI and PAAI-PnBA-PAAI we turned to dynamic mechanical analysis (DMA). Chang and Yang demonstrated the ability to directly correlate the behavior of an adhesive during tack and peel testing to the response observed during DMA at bonding and debonding frequencies, respectively.[47] Specifically, the response of the material during a bonding event correlates to a frequency of ∼1 rad s^{-1}, while debonding under standard 180° peel testing conditions roughly corresponds to higher frequencies of ∼435 rad s^{-1}. Characterizing the elastic and viscous response of the material (G' and G'', respectively) at the bonding and debonding frequencies therefore allows one to connect the observed behavior during adhesion testing to fundamental viscoelastic properties.

DOI: 10.1021/acssuschemeng.6b00455
ACS Sustainable Chem. Eng. 2016, 4, 3379−3387

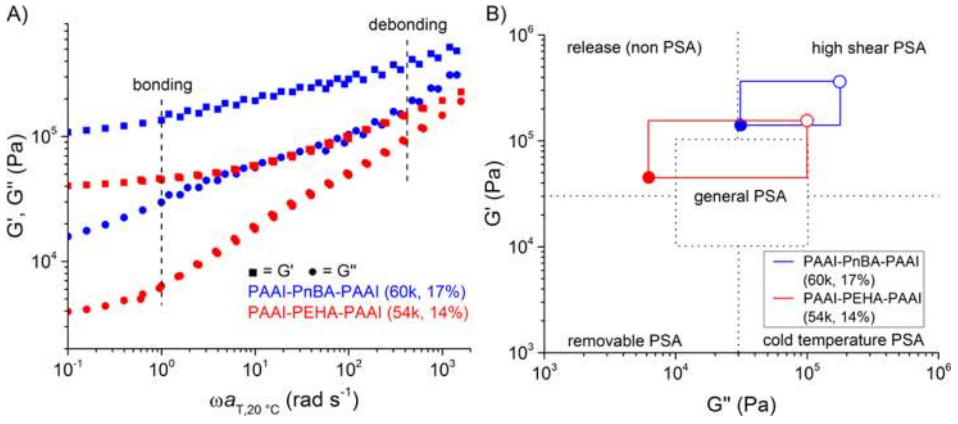

Figure 7. (A) DMA of PAAI-PnBA-PAAI (60k, 17%) and PAAI-PEHA-PAAI (54k, 14%). Bonding and debonding frequencies correspond to 1 and 435 rad s^{-1}, respectively. (B) viscoelastic windows for PAAI-PnBA-PAAI (60k, 17%) and PAAI-PEHA-PAAI (54k, 14%) constructed from bonding (●) and debonding (○) frequencies.

While a frequency of 1 rad s^{-1} is well within the typical operating range of rheometers, accessing a frequency of 435 rad s^{-1} requires employing the time temperature superposition principle (TTS). Dynamic frequency sweeps between 100 and 0.1 s^{-1} at temperatures from 20 to −20 °C were performed for PAAI-PnBA-PAAI (60k, 17%) and PAAI-PEHA-PAAI (54k, 14%). Shift factors (a_T) were then applied to generate master curves for each polymer with 20 °C as the reference temperature (Figures S35 and S36). In both cases the Williams−Landel−Ferrey model was successfully fit to the plot of $a_{T,20\ °C}$ vs temperature. It should be noted that attempts to generate a full master curve for the triblock copolymers by including dynamic frequency sweeps measured at higher temperatures were unsuccessful (Figures S37 and S38). At temperatures above 30 °C TTS could not be applied successfully, potentially due to the difference in relaxation times of the different blocks or the presence of a transition such as T_g or mixing of the PAAI and midblock components.[50]

The resulting plots of moduli vs frequency from DMA of PAAI-PnBA-PAAI (60k, 17%) and PAAI-PEHA-PAAI (54k, 14%) are shown in Figure 7. At the bonding and debonding frequencies, both G' and G'' for PAAI-PnBA-PAAI (60k, 17%) are higher than for PAAI-PEHA-PAAI (54k, 14%). This observation is in good agreement with the results from tensile testing where PAAI-PnBA-PAAI exhibited higher E than PAAI-PEHA-PAAI. Both polymer samples satisfy the Dahlquist criterion, which states that for measurable tack to occur G' should be $<3 \times 10^5$ Pa in the bonding region. However, this criterion clearly does not predict the behavior of PAAI-PEHA-PAAI (54k, 14%) as this sample registered no measurable force during loop tack testing.

Appling the viscoelastic window concept as outlined by Yang and Chang[47] allowed for a better understanding of how the viscoelastic behavior at bonding and debonding frequencies can be used to understand the difference in adhesive qualities. The viscoelastic window is constructed by plotting G' and G'' at bonding and debonding frequencies on a plot of G' vs G''. The region in which the viscoelastic window lies can then be used to qualitatively assess the behavior of the PSA and its area of application. For PAAI-PnBA-PAAI (60k, 17%) the window lies within the high shear region. PSAs with windows in this region are described as having moderate peel forces and high resistance to shear, which is in good agreement with the results from 180° peel and shear testing. By contrast, a high ratio of G' to G'' in the bonding region of PAAI-PEHA-PAAI (54k, 14%) results in a viscoelastic window that partially lies within the non-PSA region. If the ratio of G' to G'' is too high, the polymer lacks the liquid like quality needed to form intimate contact with the substrate. In other words, dissipation is low. As a result the polymer does not register a tack force during loop tack testing.

CONCLUSION

In summary, we have reported the synthesis of a new isosorbide derived monomer AAI in two steps using common reagents. PAAI had a T_g near that of commercially relevant glassy polymers such as poly(styrene) and PMMA and demonstrated good thermal stability. RAFT polymerization was used to prepare two series of triblock copolymers PAAI-PnBA-PAAI and PAAI-PEHA-PAAI with varying wt % PAAI. The adhesive qualities of the triblock copolymers were evaluated by 180° peel, loop tack, and shear testing. Results for the PAAI-PnBA-PAAI series were promising and comparable to previously reported results for PMMA-PnBA-PMMA, while rather poor adhesive qualities were observed for the PAAI-PEHA-PAAI series. DMA provided insight into the cause for the observed differences in adhesive performance, suggesting that a high ratio of G' to G'' in the bonding regime of PAAI-PEHA-PAAI limits adhesion to the substrate. Together the above results demonstrate the utility of isosorbide in thermoplastic elastomer applications and provide a robust approach to incorporating this low cost biobased feedstock into new polymer materials.

ASSOCIATED CONTENT

Supporting Information

The Supporting Information is available free of charge on the ACS Publications website at DOI: 10.1021/acssuschemeng.6b00455.

Table S1, Schemes S1 and S2, Figures S1−S49, and experimental procedures (PDF)

AUTHOR INFORMATION

Corresponding Authors

*E-mail: hillmyer@umn.edu (M.A.H.).
*E-mail: treineke@umn.edu (T.M.R.).

Notes

The authors declare no competing financial interest.

DOI: 10.1021/acssuschemeng.6b00455
ACS Sustainable Chem. Eng. 2016, 4, 3379−3387

■ ACKNOWLEDGMENTS

This work was supported by the NSF under the Center for Sustainable Polymers, CHE-1413862. Part of this work was carried out in the College of Science and Engineering Polymer Characterization Facility, University of Minnesota, which has received capital equipment funding from the NSF through the UMN MRSEC program under Award Number DMR-1420013. SAXS was performed at the DuPont−Northwestern−Dow Collaborative Access Team (DND-CAT) located at Sector 5 of the Advanced Photon Source (APS). DND-CAT is supported by E. I. du Pont de Nemours & Co., The Dow Chemical Company, and Northwestern University. Use of the APS, an Office of Science User Facility operated for the U.S. Department of Energy (DOE) Office of Science by Argonne National Laboratory, was supported by the U.S. DOE under Contract DE-AC02-06CH11357.

■ REFERENCES

(1) Gandini, A. The irruption of polymers from renewable resources on the scene of macromolecular science and technology. *Green Chem.* **2011**, *13*, 1061−1083.
(2) Delidovich, I.; Hausoul, P. J. C.; Deng, L.; Pfützenreuter, R.; Rose, M.; Palkovits, R. Alternative Monomers Based on Lignocellulose and Their Use for Polymer Production. *Chem. Rev.* **2016**, *116*, 1540−1599.
(3) Isikgor, F. H.; Remzi Becer, C. Lignocellulosic Biomass: a sustainable platform for production of bio-based chemicals and polymers. *Polym. Chem.* **2015**, *6*, 4497−4559.
(4) Holmberg, A. L.; Reno, K. H.; Wool, R. P.; Epps, T. H. I. Biobased building blocks for the rational design of renewable block polymers. *Soft Matter* **2014**, *10*, 7405−7424.
(5) Scott, A. Roquette embraces biobased materials. *C&EN* **2014**, *90*, 16−17.
(6) *ROQUETTE reinforces its position as world leader in ISOSORBIDE for the performance plastics and chemistry markets*; ROQUETTE, 2015.
(7) Fenouillot, F.; Rousseau, A.; Colomines, G.; Saint-Loup, R.; Pascault, J. P. Polymers from renewable 1,4:3,6-dianhydrohexitols (isosorbide, isomannide and isoidide): A review. *Prog. Polym. Sci.* **2010**, *35*, 578−622.
(8) Rose, M.; Palkovits, R. Isosorbide as a renewable platform chemical for versatile applications−quo vadis? *ChemSusChem* **2012**, *5*, 167−176.
(9) Galbis, J. A.; García-Martín, M. G. Synthetic polymers from readily available monosaccharides. *Top. Curr. Chem.* **2010**, *295*, 147−176.
(10) Mitsubishi Chemical. World-First—DURABIO, Bio-based Engineering Plastic from Mitsubishi Chemical, Used on the Front Panel of Sharp's New AQUOS CRYSTAL 2 Smartphone. http://www.m-kagaku.co.jp/english/newsreleases/00258.html (accessed Mar 23, 2016).
(11) Mitsubishi Chemical. New biobased engineering plastic "DURABIO". http://www.m-kagaku.co.jp/english/products/business/polymer/sustainable/details/1194667_3255.html (accessed Mar 23, 2016).
(12) Gallagher, J. J.; Hillmyer, M. A.; Reineke, T. M. Isosorbide-based Polymethacrylates. *ACS Sustainable Chem. Eng.* **2015**, *3*, 662−667.
(13) Beghdadi, S.; Miladi, I. A.; Ben Romdhane, H.; Bernard, J.; Drockenmuller, E. RAFT polymerization of bio-based 1-vinyl-4-dianhydrohexitol-1,2,3-triazole stereoisomers obtained via click chemistry. *Biomacromolecules* **2012**, *13*, 4138−4145.
(14) Sato, K.; Kodama, K. Positive-working far-UV photoresists. JP 2004341062, 2004.
(15) Koyama, H.; Tsutsumi, K. Polymerizable monomer polymeric compound resin compositions for photoresist and method for producing semiconductor. wo 2004113404, 2004.
(16) Mansoori, Y.; Hemmati, S.; Eghbali, P.; Zamanloo, M. R.; Imanzadeh, G. Nanocomposite materials based on isosorbide methacrylate/Cloisite 20A. *Polym. Int.* **2013**, *62*, 280−288.
(17) Bates, F. S.; Fredrickson, G. H. Block Copolymers—Designer Soft Materials. *Phys. Today* **1999**, *52*, 32−38.
(18) Creton, C. Pressure-Sensitive Adhesives: An Introductory Course. *MRS Bull.* **2003**, *28*, 434−439.
(19) Moineau, C.; Minet, M.; Teyssié, P.; Jérôme, R. Synthesis and Characterization of Poly(methyl methacrylate)-block-poly(n-butyl acrylate)-block-poly(methyl methacrylate) Copolymers by Two-Step Controlled Radical Polymerization (ATRP) Catalyzed by NiBr2 (PPh3)2, 1†. *Macromolecules* **1999**, *32*, 8277−8282.
(20) Tong, J. D.; Jerôme, R. Synthesis of poly(methyl methacrylate)-b-poly(n-butyl acrylate)-b-poly(methyl methacrylate) triblocks and their potential as thermoplastic elastomers. *Polymer* **2000**, *41*, 2499−2510.
(21) Haloi, D. J.; Ata, S.; Singha, N. K.; Jehnichen, D.; Voit, B. Acrylic AB and ABA block copolymers based on poly(2-ethylhexyl acrylate) (PEHA) and poly(methyl methacrylate) (PMMA) via ATRP. *ACS Appl. Mater. Interfaces* **2012**, *4*, 4200−4207.
(22) Dufour, B.; Koynov, K.; Pakula, T.; Matyjaszewski, K. PBA−PMMA 3-Arm Star Block Copolymer Thermoplastic Elastomers. *Macromol. Chem. Phys.* **2008**, *209*, 1686−1693.
(23) Oshita, S.; Chapman, B. K.; Hirata, K. Acrylic Block Copolymer for Adhesive Application. In *PSTC Tape Summit 2012*, Boston, 2012.
(24) Hamada, K.; Ishiura, K.; Takahashi, T.; Yaginuma, S.; Akai, M.; Ono, T.; Shachi, K. Process for polymerizing a methacrylic ester or an acrylic ester. US 6,767,976 B2, 2004.
(25) Brandrup, J.; Immergut, E.; Grulke, E.; Abe, A.; Bloch, D. *Polymer handbook*, 4th ed.; Wiley, 1999; Vol. *49*.
(26) Vendamme, R.; Schüwer, N.; Eevers, W. Recent synthetic approaches and emerging bio-inspired strategies for the development of sustainable pressure-sensitive adhesives derived from renewable building blocks. *J. Appl. Polym. Sci.* **2014**, *131*, 8379−8394.
(27) Lee, S.; Lee, K.; Kim, Y.-W.; Shin, J. Preparation and Characterization of a Renewable Pressure-Sensitive Adhesive System Derived from ε-Decalactone, L-Lactide, Epoxidized Soybean Oil, and Rosin Ester. *ACS Sustainable Chem. Eng.* **2015**, *3*, 2309−2320.
(28) Ding, K.; John, A.; Shin, J.; Lee, Y.; Quinn, T.; Tolman, W. B.; Hillmyer, M. A. High-Performance Pressure-Sensitive Adhesives from Renewable Triblock Copolymers. *Biomacromolecules* **2015**, *16*, 2537−2539.
(29) Shin, J.; Martello, M. T.; Shrestha, M.; Wissinger, J. E.; Tolman, W. B.; Hillmyer, M. A. Pressure-Sensitive Adhesives from Renewable Triblock Copolymers. *Macromolecules* **2011**, *44*, 87−94.
(30) Shin, J.; Lee, Y.; Tolman, W. B.; Hillmyer, M. A. Thermoplastic elastomers derived from menthide and tulipalin A. *Biomacromolecules* **2012**, *13*, 3833−3840.
(31) Gu, C.; Dubay, M. R.; Severtson, S. J.; Gwin, L. E. Hot-Melt Pressure-Sensitive Adhesives Containing High Biomass Contents. *Ind. Eng. Chem. Res.* **2014**, *53*, 11000−11006.
(32) Pu, G.; Hauge, D. A.; Gu, C.; Zhang, J.; Severtson, S. J.; Wang, W.; Houtman, C. J. Influence of Acrylated Lactide-Caprolactone Macromonomers on the Performance of High Biomass Content Pressure-Sensitive Adhesives. *Macromol. React. Eng.* **2013**, *7*, 515−526.
(33) Pu, G.; Dubay, M. R.; Zhang, J.; Severtson, S. J.; Houtman, C. J. Polyacrylates with high biomass contents for pressure-sensitive adhesives prepared via mini-emulsion polymerization. *Ind. Eng. Chem. Res.* **2012**, *51*, 12145−12149.
(34) Vendamme, R.; Eevers, W. Sweet Solution for Sticky Problems: Chemoreological Design of Self-Adhesive Gel Materials Derived From Lipid Biofeedstocks and Adhesion Tailoring via Incorporation of Isosorbide. *Macromolecules* **2013**, *46*, 3395−3405.
(35) Stoss, P.; Merrath, P.; Schlüter, G. Regioselektive Acylierung von 1,4:3,6-Dianhydro-D-glucit. *Synthesis* **1987**, *1987*, 174−176.
(36) Stoss, P. Process for the production of isosorbide-5-nitrate. US 4,371,703, 1983.

DOI: 10.1021/acssuschemeng.6b00455
ACS Sustainable Chem. Eng. 2016, 4, 3379−3387

(37) Beyler, C. L.; Hirschler, M. M. Thermal Decomposition of Polymers. In *SFPE Handbook of Fire Protection Engineering*; DiNenno, P. J., Ed.; 2001; pp 110−131.
(38) Mahalik, J. P.; Madras, G. Effect of the Alkyl Group Substituents on the Thermal and Enzymatic Degradation of Poly(n-alkyl acrylates). *Ind. Eng. Chem. Res.* **2005**, *44*, 4171−4177.
(39) Moad, G.; Rizzardo, E.; Thang, S. H. Living Radical Polymerization by the RAFT Process - A Third Update. *Aust. J. Chem.* **2012**, *65*, 985−1076.
(40) Keddie, D. J. A guide to the synthesis of block copolymers using reversible-addition fragmentation chain transfer (RAFT) polymerization. *Chem. Soc. Rev.* **2014**, *43*, 496−505.
(41) Perrier, S.; Barner-Kowollik, C.; Quinn, J. F.; Vana, P.; Davis, T. P. Origin of Inhibition Effects in the Reversible Addition Fragmentation Chain Transfer (RAFT) Polymerization of Methyl Acrylate. *Macromolecules* **2002**, *35*, 8300−8306.
(42) Malic, N.; Evans, R. A. Synthesis of Carboxylic Acid and Ester Mid-Functionalized Polymers using RAFT Polymerization and ATRP. *Aust. J. Chem.* **2006**, *59*, 763−771.
(43) Ohara, T.; Sato, T.; Shimizu, N.; Prescher, G.; Schwind, H.; Weiberg, O.; Marten, K.; Greim, H. Acrylic Acid and Derivatives. In *Ullmann's Encyclopedia of Industrial Chemistry*; Wiley-VCH Verlag GmbH & Co. KGaA: Weinheim, Germany, 2000; Vol. *60*, pp 1−18.
(44) Tullo, A. H. Hunting For Biobased Acrylic Acid. *Chem. Eng. News* **2013**, *91*, 18−19.
(45) Kavitha, A. A.; Singha, N. K. Smart "all acrylate" ABA triblock copolymer bearing reactive functionality via atom transfer radical polymerization (ATRP): Demonstration of a "click reaction" in thermoreversible property. *Macromolecules* **2010**, *43*, 3193−3205.
(46) Nakamura, Y.; Adachi, M.; Tachibana, Y.; Sakai, Y.; Nakano, S.; Fujii, S.; Sasaki, M.; Urahama, Y. Tack and viscoelastic properties of an acrylic block copolymer/tackifier system. *Int. J. Adhes. Adhes.* **2009**, *29*, 806−811.
(47) Yang, H. W. H.; Chang, E.-P. The role of viscoelastic properties in the design of pressure-sensitive adhesives. *Trends Polym. Sci.* **1997**, *5*, 380−384.
(48) Fiebach, K.; Grimm, D. Resins, Natural. In *Ullmann's Encyclopedia of Industrial Chemistry*; Wiley-VCH Verlag GmbH & Co. KGaA: Weinheim, Germany, 2000; Vol. *9*, pp 245−260.
(49) Benedek, I. *Pressure-Sensitive Adhesives and Applications*; CRC Press, 2004.
(50) Hiemenz, P. C.; Lodge, T. P. *Polymer Chemistry*, Second ed.; Taylor & Francis, 2007.

DOI: 10.1021/acssuschemeng.6b00455
ACS Sustainable Chem. Eng. 2016, 4, 3379−3387